

Rapid Ocular Dominance Plasticity Requires Cortical but Not Geniculate Protein Synthesis

Sharif Taha and Michael P. Stryker¹

W.M. Keck Foundation Center for
Integrative Neuroscience and
Department of Physiology
University of California, San Francisco
San Francisco, California 94143

Summary

Synaptic plasticity is a multistep process in which rapid, early phases eventually give way to slower, more enduring stages. Diverse forms of synaptic change share a common requirement for protein synthesis in the late stages of plasticity, which are often associated with structural rearrangements. Ocular dominance plasticity in the primary visual cortex (V1) is a long-lasting form of activity-dependent plasticity comprised of well-defined physiological and anatomical stages. The molecular events underlying these stages remain poorly understood. Using the protein synthesis inhibitor cycloheximide, we investigated a role for protein synthesis in ocular dominance plasticity. Suppression of cortical, but not geniculate, protein synthesis impaired rapid ocular dominance plasticity, while leaving neuronal responsiveness intact. These findings suggest that structural changes underlying ocular dominance plasticity occur rapidly following monocular occlusion, and cortical changes guide subsequent alterations in thalamocortical afferents.

Introduction

The molecular events underlying different forms of activity-dependent synaptic change show remarkable stereotypy in their progression: plasticity is generally composed of distinct, often sequential, stages in which the transition from early to late stages is marked by a dependence on protein synthesis (Bailey et al., 1996; Dubnau and Tully, 1998; Levenes et al., 1998; Mayford and Kandel, 1999). The sensitivity of late stages of plasticity to disruption by protein synthesis inhibitors was first demonstrated in studies of memory formation *in vivo*, where injections of puromycin in mice were shown to disrupt long-term, but not short-term, expression of learned maze sequences (Flexner et al., 1963). Subsequent investigations have shown that a similar requirement exists in the late stages of sensitization of the gill withdrawal reflex in *Aplysia* (Bailey et al., 1992) and multiple forms of long-term potentiation (LTP) (Krug et al., 1984; Frey et al., 1988; Kurontani et al., 1996; Barea-Rodríguez et al., 2000) and long-term depression (Linden, 1996; Huber et al., 2000). In each case, short-term expression of plasticity is thought to require only covalent modifications of existing proteins, while long-term changes require new protein synthesis.

Protein synthesis is thought to be necessary for struc-

tural rearrangements at the synapse, and studies in systems that provide accessible anatomical preparations support this view. In *Aplysia*, for instance, the time course of the development of long-term sensitization of the gill withdrawal reflex is paralleled by an increase in the number of synaptic varicosities in sensory neurons and structural rearrangements in synaptic active zones (Bailey and Chen, 1989). Moreover, these structural changes share with long-term sensitization a requirement for ongoing protein synthesis (Bailey et al., 1992).

The findings described above suggest that protein synthesis is a molecular gateway—an early and necessary molecular step—to long-term plasticity, driven by structural rearrangements at the synapse. The developing visual cortex is an experimental system in which the time course of distinct physiological and anatomical substrates of plasticity has been well studied, and hence, provides the opportunity to investigate the molecular correlates of these changes. During a discrete critical period in postnatal development, synapses in the V1 are exceptionally plastic, such that brief periods of monocular deprivation (MD) induce robust changes in the balance of the two eyes' input to cortex (Wiesel and Hubel, 1963; Olson and Freeman, 1980). In the mouse, the effects of MD are evident in electrophysiological recordings after 4 days of MD (Gordon and Stryker, 1996). Anatomical changes in thalamocortical arbors require substantially longer periods of deprivation for full expression (Antonini et al., 1999).

Little is known about the molecular mechanisms that underlie ocular dominance plasticity. In particular, the events required for initiating long-lasting changes at the synapse remain enigmatic. N-methyl-D-aspartate receptor function is required for ocular dominance plasticity (Bear et al., 1990; Roberts et al., 1998), as is the kinase action of the synaptic protein α calcium-calmodulin kinase II (α CaMKII) (Gordon et al., 1996); both molecules are likely to be involved in early stages of plasticity induction, given their well-defined roles in mediating neuronal calcium influx (Daw et al., 1993) and initiating calcium-dependent signaling (Soderling, 2000). Downstream signaling events are not well understood, but the many documented examples of activity-dependent protein synthesis suggest that translation of proteins is required for normal plasticity. Multiple plasticity-related genes show visually driven increases in protein levels, including α CaMKII (Wu et al., 1998) and the calcium/cyclicAMP-response element binding protein (Pham et al., 1999), and lengthy MD can alter gross levels of protein synthesis in the lateral geniculate nucleus (LGN) (Kennedy et al., 1981). Neurotrophins and their receptors are regulated in an activity-dependent fashion *in vitro* and *in vivo* (Zafra et al., 1992; Schoups et al., 1995; Androutsellis-Theotokis et al., 1996; Lein and Shatz, 2000) and have potent effects upon synaptic plasticity in the visual cortex (Cabelli et al., 1995; McAllister et al., 1995; Hanover et al., 1999; Gillespie et al., 2000). To date, however, there has been no direct demonstration of a requirement for protein synthesis in ocular dominance plasticity.

¹Correspondence: stryker@phy.ucsf.edu

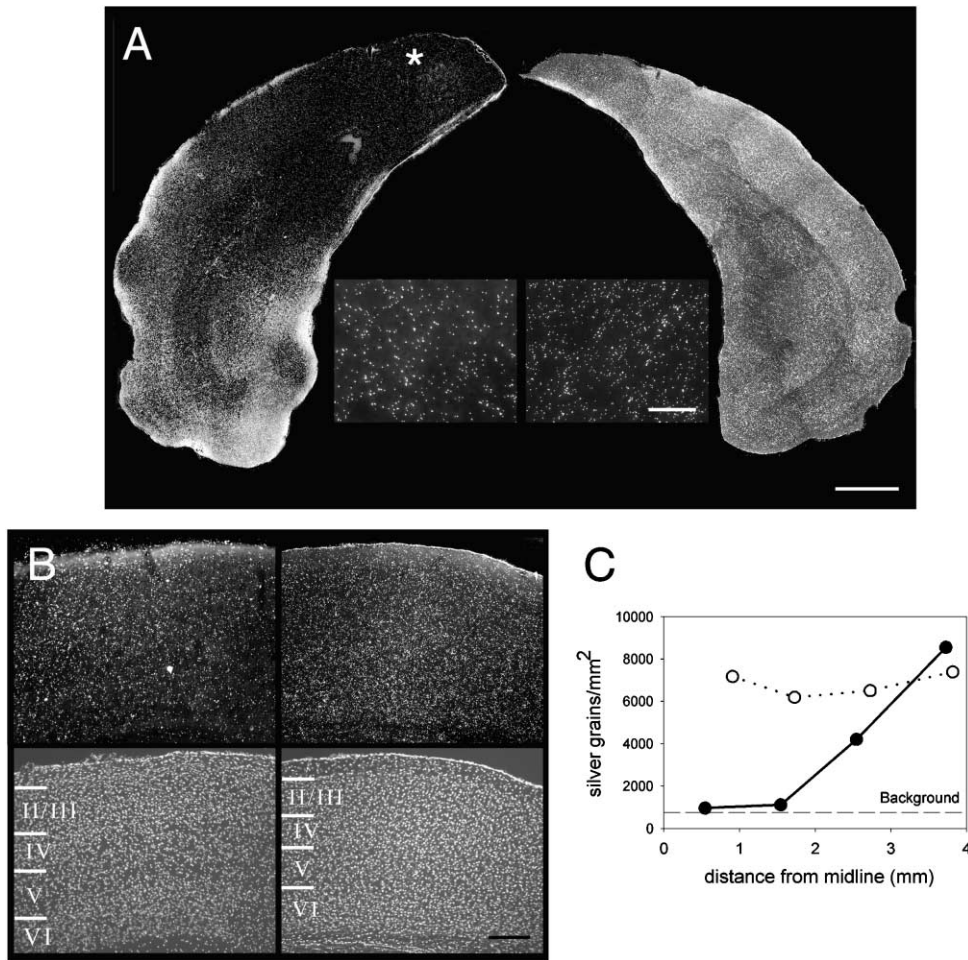


Figure 1. Cortical Cycloheximide Infusion Blocks Protein Synthesis Locally

(A) Coronal sections through V1 show suppression of protein synthesis in the infused hemisphere (left, with mediolateral position of cannula indicated by the asterisk), but not the uninfused hemisphere (right). High-magnification insets show silver grains in the region of V1 (~2 mm from the midline in this section); the silver grain count in uninfused V1 (right inset) is approximately 2-fold higher than that in cycloheximide-infused V1 (left inset). Scale bar, 1 mm; inset scale bar, 100 μ m.

(B) Silver grains representing protein synthesis in cycloheximide-infused (top left) and uninfused (top right) coronal sections, with nuclear bisbenzamide staining from identical sections (below) showing cortical laminae in V1. Sections are the same as those shown in (A). Scale bar, 200 μ m.

(C) Quantification of silver grain density over the medial-lateral extent of the cycloheximide-infused (closed symbols) and uninfused (open symbols) sections shown in (A).

To investigate this issue, we infused the protein synthesis inhibitor cycloheximide into distinct neural targets, while subjecting mice to concurrent MD. We demonstrate that intact levels of protein synthesis are necessary for ocular dominance plasticity and that this requirement for translation arises rapidly after monocular occlusion. The locus of this requirement is cortical; while thalamic inhibition of protein synthesis leaves ocular dominance plasticity intact, cortical infusions of cycloheximide block the effects of MD.

Results

Inhibition of Protein Synthesis in Visual Cortex

Monocular deprivation in mice must be maintained over 4 days to induce expression of near saturating plasticity (Gordon and Stryker, 1996). Thus, it was necessary to

establish a reliable means of inhibiting protein synthesis in the visual cortex over a period of days. We used osmotic minipumps to infuse cycloheximide directly into cortical tissue medial to V1, choosing a concentration that minimized neurotoxic effects of the drug but that was sufficient to suppress protein synthesis several millimeters from the infusion site.

A typical example of the effects of extended (5 day) unilateral infusion of cycloheximide is shown in a coronal slice of mouse brain in Figure 1A. Protein synthesis in the region of the visual cortex, as measured by incorporation of the tritium-labeled amino acid leucine into nascent proteins (see Experimental Procedures), was substantially suppressed in the CYC-infused hemisphere. Silver grain density decreased in a lateral to medial gradient in the CYC-infused hemisphere, reflecting the medial placement of the infusion cannula. Protein synthesis

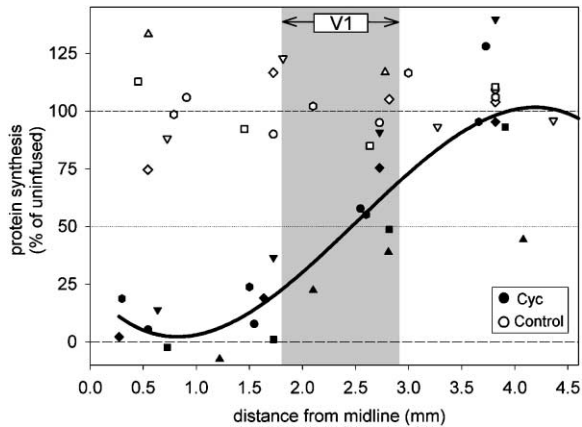


Figure 2. Cortical Cycloheximide Infusion Reliably Suppresses Protein Synthesis in V1

Protein synthesis is significantly suppressed over the span of V1 (gray strip) in cycloheximide-infused hemispheres ($n = 6$; closed symbols) relative to protein synthesis levels in uninfused hemispheres ($n = 6$; open symbols). The regression line (black line; $r^2 = 0.78$) fitted to data from cycloheximide-infused hemispheres shows protein synthesis is significantly suppressed relative to saline-infused controls ($p < 0.0001$). Different symbols represent data taken from individual animals.

levels in the uninfused hemisphere were uniformly high across the medial-lateral span of the cortex, indicating that little, if any, cycloheximide crossed the midline. High-magnification insets show silver grain puncta in the region of the visual cortex.

The spatial gradient of protein synthesis inhibition was quantified by sampling silver grain counts across the medial-lateral extent of the hemisphere (Figure 1C; results from section shown in Figure 1A). In the infused hemisphere, protein synthesis was reduced to near background levels close to the midline, remained substantially inhibited 2–3 mm away, and rose to control levels near 4 mm from the midline. Protein synthesis levels varied only slightly across the extent of the uninfused hemisphere.

A side by side comparison of infused and uninfused bisbenzimid-stained sections (Figure 1B) shows that cycloheximide infusion did not disrupt the normal laminar structure of the cortex nor reduce cell density (cell density in infused V1 = $93\% \pm 6\%$ of uninfused V1; $p = 0.42$; t test) in the region of the visual cortex. These properties of normal cortical architecture were maintained despite substantial suppression of protein synthesis; in the region shown, silver grain density in the CYC-infused hemisphere was reduced approximately 2-fold relative to the uninfused hemisphere.

Grouped results taken from multiple unilateral cortical infusions ($n = 6$ mice) are shown in Figure 2. Silver grain counts were normalized to the average silver grain density in all uninfused hemispheres and plotted as a function of distance from the midline. Using cytoarchitectonic cues, V1 was located in infused hemispheres: the gray strip indicates the position of V1 relative to the midline (medial margin of V1 = 1.8 ± 0.2 mm from midline; lateral margin = 2.9 ± 0.2 mm). On average, our infusion protocol reduced protein synthesis in V1 to less

than half that measured in uninfused hemispheres ($45\% \pm 12\%$ at midpoint of V1, mean \pm 95% confidence interval). Though there was variability in the extent of protein synthesis inhibition, all infused hemispheres showed significantly reduced protein synthesis near the medial margin of V1 (avg = $18\% \pm 5.1\%$ of uninfused mean at 1.70 ± 0.09 mm from midline; $p < 0.001$; t test). Near the lateral margin of V1, protein synthesis was somewhat higher ($61\% \pm 7.7\%$ at 2.7 ± 0.04 mm), but was still significantly reduced relative to control levels ($p < 0.05$; t test). Thus, our infusion protocol yielded a reliable means of suppressing protein synthesis in the region of the V1.

Blockade of Ocular Dominance Plasticity after Cortical Protein Synthesis Inhibition

Having established the effectiveness of cycloheximide infusion in suppressing protein synthesis, we tested the effects of such inhibition upon ocular dominance plasticity. Lid suture was performed at the peak of the critical period, between p26 and p30, and MD lasted 4 days in all cases. Mice were implanted with minipumps for cycloheximide infusion 1 day prior to lid suture, and infusion was continued over the 4 days of MD. Ocular dominance was measured using extracellular single unit recordings of visual responses in binocular visual cortex. For purposes of comparison, units from each mouse were used to compute a single contralateral bias index (CBI), which reflects the relative strength of the contralateral eye's input to cortex.

In normal mice, cortical responses are dominated by the contralateral eye. This is reflected in the high mean CBI of nondeprived mice (CBI = 0.75 ± 0.03 , mean \pm SEM; Figure 3A) and the left-shifted distribution of units in the ocular dominance histogram (Figure 3B). Control mice infused with physiological saline 1 day prior to, and concurrent with 4 days of MD, displayed a robust shift in ocular dominance, such that the balance of neuronal responses came to favor the nondeprived ipsilateral eye (CBI = 0.46 ± 0.01 ; Figure 3A). The shift in the distribution of ocular dominance scores of individual units following saline + MD treatment can be seen in Figure 3C. The dotted line is a best fit for the distribution of ocular dominance scores in normal, nondeprived animals; following saline infusion + MD, responses shifted significantly ($p < 0.0001$; t test) toward the open ipsilateral eye.

Infusion of cycloheximide blocked the normal effects of MD. The mean CBI of animals undergoing cycloheximide + MD treatment (CBI = 0.70 ± 0.04) was similar to that of nondeprived animals ($p = 0.36$; t test), but significantly different from that of the saline + MD group ($p < 0.005$; t test). The majority of neurons in CYC-infused animals continued to be driven by the deprived contralateral eye, and as can be seen in Figure 3D, the distribution of ocular dominance scores following cycloheximide infusion remained very similar to that observed in nondeprived animals.

The effects of protein synthesis inhibition on ocular dominance plasticity were consistent across the mediolateral extent of the recording sites in binocular V1. The mean CBI value calculated from penetrations made near the cannula (CBI_{near} = 0.70; 6 penetrations and 41 units) did

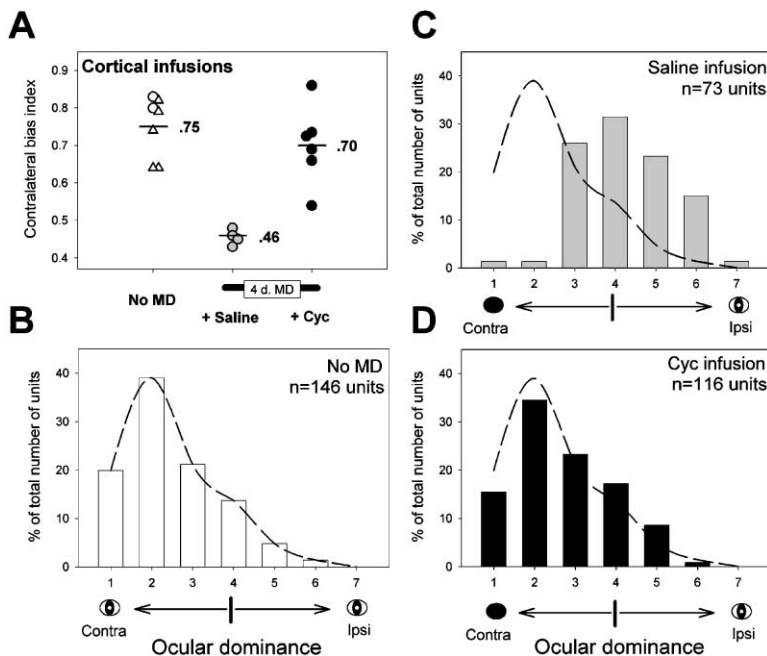


Figure 3. Inhibition of Cortical Protein Synthesis Blocks Ocular Dominance Plasticity

(A) Normal, nondeprived mice show a strong contralateral bias ($n = 7$ mice; open symbols; triangles shown noncritical period age mice; see Experimental Procedures). After 4 day MD, saline-infused animals shift toward the open ipsilateral eye ($n = 4$; gray symbols), but cycloheximide-infused animals ($n = 6$; closed symbols) do not. Mean CBI for each group is indicated to the right of horizontal bars.

(B) The histogram of single units recorded from normal, nondeprived mice is weighted heavily toward the contralateral eye. A smoothed curve (broken line) was fitted to the data for purposes of comparison with (C) and (D) below.

(C and D) Histograms of saline- (C) and cycloheximide-infused (D) animals showing ocular dominance scores of single units recorded from animals shown in (A). The dashed line in both panels shows the distribution of ocular dominance scores for the nondeprived mice shown in (A); the left-shifted peak reflects the contralateral bias found in normal mice. MD + saline infusion (gray bars) results in a relative increase in cortical responses driven by the ipsilateral eye and a pronounced shift toward

higher ocular dominance scores. Plasticity is blocked in cycloheximide-infused animals (black bars); units recorded from these mice continue to be driven by the closed contralateral eye, and their distribution remains similar to nondeprived animals.

not differ from that derived from penetrations made far from the cannula ($CBI_{far} = 0.68$; 6 penetrations and 37 units; mean separation of “near” and “far” penetrations = $478 \mu\text{m}$), suggesting threshold levels of protein synthesis inhibition necessary to block plasticity were reached in all portions of primary visual cortex.

Single Unit Responses in CYC-Infused V1

Ocular dominance plasticity is critically dependent upon cortical levels of neuronal responsiveness (Shaw and Cynader, 1984; Reiter et al., 1986; Reiter and Stryker, 1988; Hensch et al., 1998). To ensure that CYC infusion did not alter neuronal responsiveness, we quantified a number of single unit response properties. The frequency with which isolated units were encountered in CYC- and saline-infused animals did not differ (CYC-infused mean \pm SD = $79 \pm 47 \mu\text{m}$, saline-infused mean = $78 \pm 19 \mu\text{m}$; $p = 0.84$; t test), suggesting that the number of visually responsive neurons was not altered by protein synthesis inhibition. Quantitative analysis of single unit responses showed that the magnitude of neuronal responses was also unaltered by CYC infusion, as levels of stimulus-driven (CYC-infused mean = 3.57 ± 0.38 spikes/s; saline-infused mean = 3.64 ± 0.43 spikes/s; $p = 0.90$; t test) and spontaneous activity (CYC-infused mean = 0.26 ± 0.08 spikes/s; saline-infused mean = 0.26 ± 0.05 spikes/s; $p = 0.98$; t test) were similar in both groups of animals (Figure 4A). Additionally, response latencies following visual stimulus presentation were similar in the two groups, with peak neural responses occurring 25–75 ms following stimulus onset (Figure 4B).

Though our experiments indicated that single unit responses were not altered by CYC infusion, it remained

possible that other aspects of receptive field properties were impaired. However, quantification of many receptive field properties measured using single unit recording, including retinotopy, orientation bias, receptive field area, and habituation, did not reveal any changes in receptive field structure or organization (Figures 4C–4F; infused versus uninfused cortex, all $p > 0.05$; t test).

Magnitude and Precision of Neural Responses in CYC-Infused V1

To investigate potential changes in neuronal responses induced by CYC infusion, we employed two additional, quantitative techniques free of the potential biases present in single unit measures of neuronal responses (such as selection bias in isolating units). We recorded visually evoked potentials (VEP) to obtain a measure of the grouped response of a population of neurons and performed optical imaging of intrinsic signals to measure the precision of retinotopic mapping across the visual cortex.

VEPs provide a measure of the integrated response of a population of neurons, and as such, allowed a useful means of quantifying neuronal response properties. VEP waveforms varied as a function of cortical depth in a manner that was similar in CYC- and saline-infused animals (Figure 5A), typically reaching maximal amplitude $400 \mu\text{m}$ below the cortical surface. Mean peak-to-trough VEP magnitudes in the binocular region of V1 did not differ between the two groups (Figure 5B; CYC-infused mean = $95.6 \pm 15.1 \mu\text{V}$; saline-infused mean = $92.9 \pm 4.7 \mu\text{V}$; $p = 0.79$; paired t test).

We used optical imaging of intrinsic signal responses to measure the precision of retinotopic mapping in visual cortex. Mice were imaged after receiving 5 day bilateral

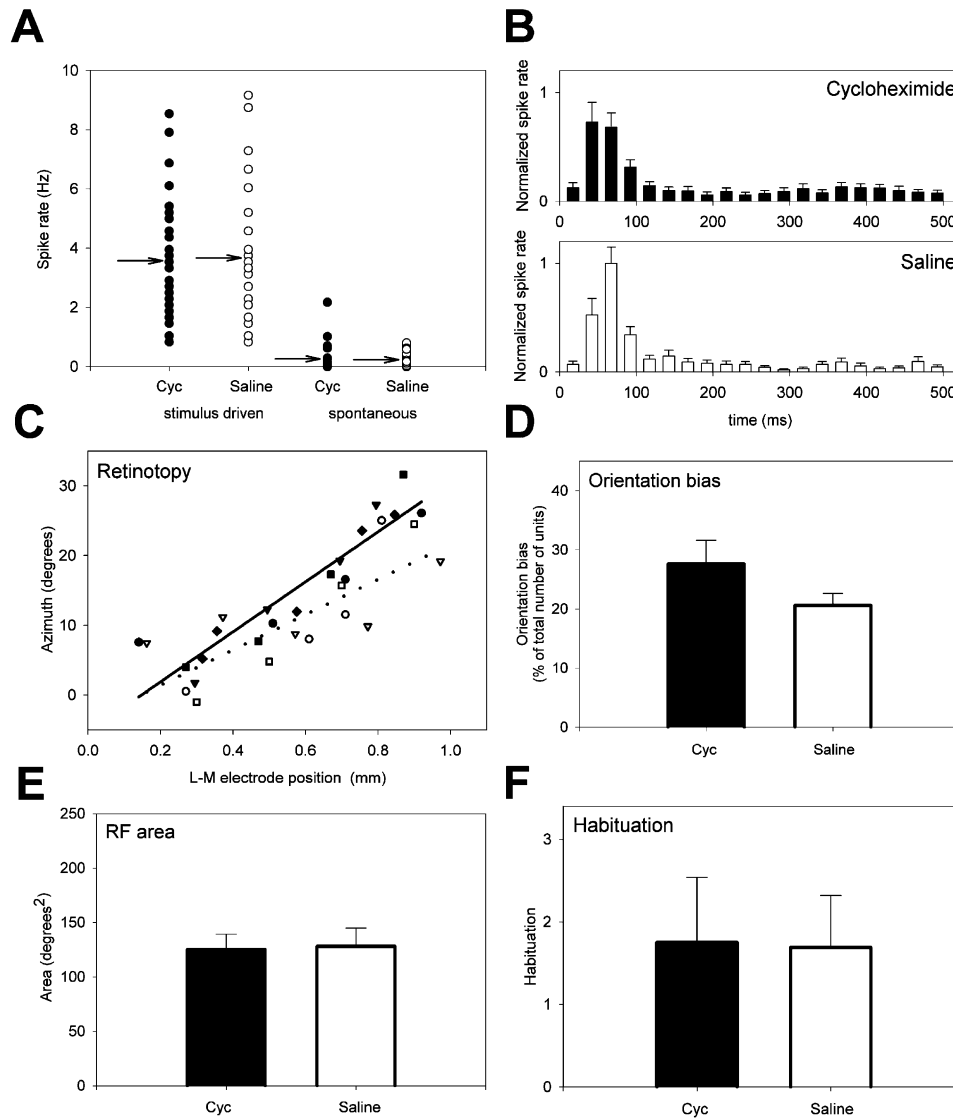


Figure 4. Single Unit Responses Are Normal in Cycloheximide-Infused Mice

(A) Mean (arrows) stimulus-driven and spontaneous firing rates did not differ between CYC- and saline-infused groups. Each symbol represents the firing rate for a single neuron (cycloheximide infused, $n = 29$ units from three mice; saline infused, $n = 26$ units from three mice). (B) Latency to firing from stimulus onset is similar in CYC- and saline-infused mice: same neurons as shown in (A). (C) Retinotopy in cycloheximide- ($n = 18$ penetrations in four hemispheres; closed symbols; unbroken line is linear best fit) and saline-infused animals ($n = 13$ penetrations in three hemispheres; open symbols; dotted line is linear best fit) is similar ($p = 0.52$, comparing slopes between groups; t test). (D) Orientation bias in single units recorded in cycloheximide- ($28\% \pm 4\%$ of total number of units, six animals, $n = 116$ units) and saline-infused ($21\% \pm 2\%$, four animals, $n = 73$ units) animals does not differ ($p = 0.18$; t test). (E) Receptive field area does not differ between groups ($p = 0.89$; t test). Mean value \pm SEM is 125.0 ± 14 degrees² in cycloheximide-infused animals ($n = 14$ units from three mice) and 128.1 ± 17 degrees² in saline-infused animals ($n = 18$ units in four animals). (F) Habituation is similar between groups (cycloheximide-infused mean \pm SEM: 1.75 ± 0.07 ; $n = 116$ units from 6 mice; saline-infused mean \pm SEM: 1.69 ± 0.07 ; $n = 73$ units from four mice; $p = 0.56$; t test).

infusions, with CYC delivered to one hemisphere and saline to the other hemisphere. Figure 5C shows the vascular pattern at the cortical surface, with saline (left hemisphere) and CYC infusion sites (red circles) visible near the midline. Figure 5D shows retinotopic mapping across the cortical surface obtained in the same animal after visual stimulus presentation. As is clear by comparison of retinotopic maps in the CYC- and saline-infused hemispheres, 5 days of CYC infusion did not alter the

normal precision of retinotopic mapping across the anterior-posterior axis of the cortex. In both hemispheres, retinotopy is mapped smoothly and continuously across the visual cortex, with the most superior elevations present in caudal portions of the cortex. While the precision of retinotopic mapping in visual cortex was not altered in CYC-infused hemispheres ($n = 6$), the magnitude of responses was slightly reduced relative to saline-infused control hemispheres ($p = 0.04$; paired t test). As both

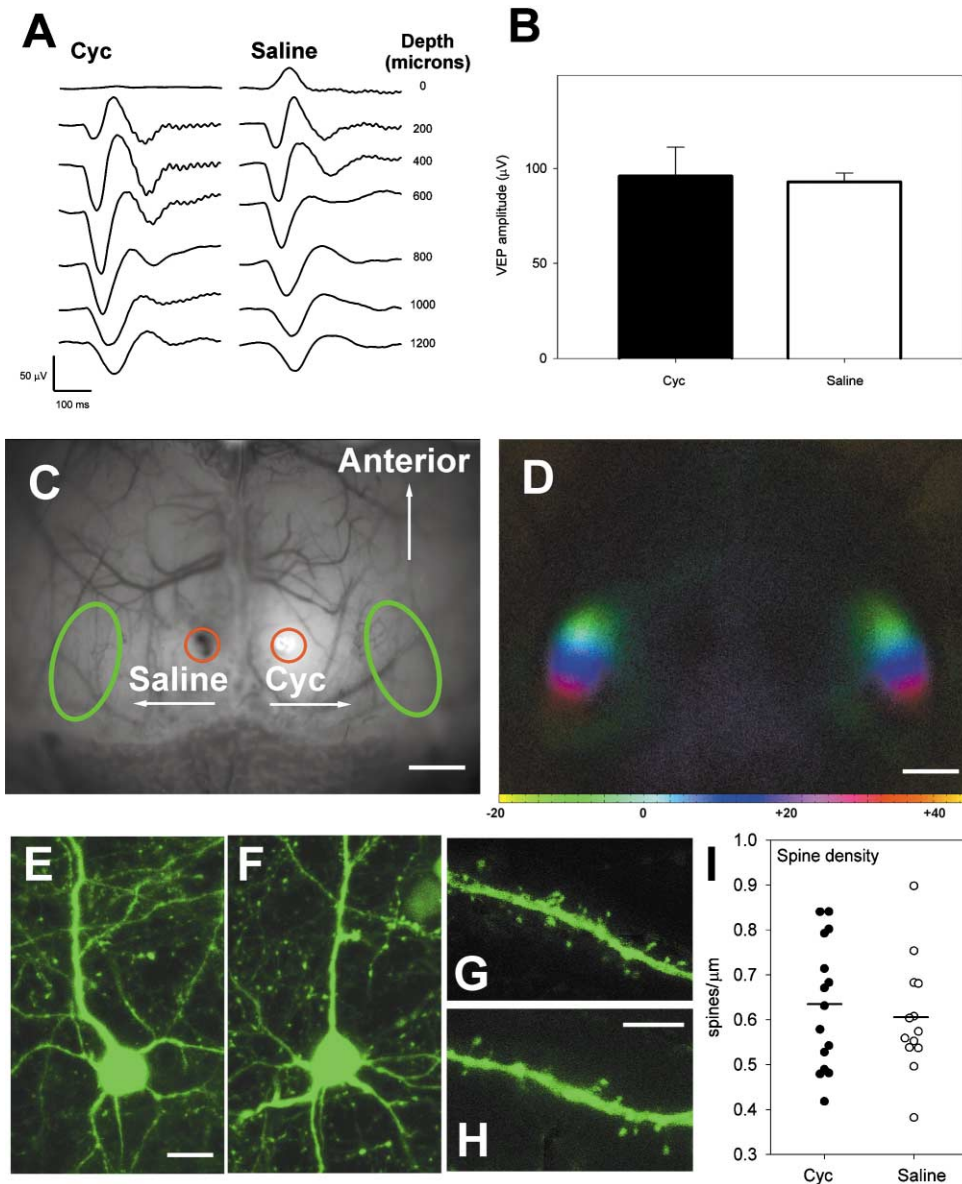


Figure 5. VEP Magnitude, Cortical Maps, and Neuronal Morphology Are Unaltered in Cycloheximide-Infused Mice

(A) VEP waveforms varied as a function of depth, reaching maximal amplitude \sim 400 μ m below the cortical surface. Representative traces shown were derived from a single mouse.

(B) Mean peak-to-trough VEP amplitude measured at a depth of 400 μ m was similar in CYC- and saline-infused animals.

(C) Infusion sites (red circles) are visible in this image of the vascular structure of the dorsal surface of the mouse brain. Cycloheximide was infused in the right hemisphere and saline in the left hemisphere; orientation of the cannula bevel directed infusions laterally toward visual cortex (green ovals), in the directions shown by the arrows. Scale bar, 1 mm.

(D) Intrinsic signal responses derived from the brain shown in (C) reveal symmetrical, precisely arranged retinotopic organization. The lightness of each pixel reflects response magnitude; dark areas are not responsive to visual stimulation. Color scale in degrees of elevation shown below.

(E and F) Projections of serial confocal optical sections taken of GFP-expressing layer V pyramidal neurons in CYC- (E) and saline-infused (F) cortices. The scale of the two images is identical. Scale bar in (E), 10 μ m.

(G and H) High-power serial confocal optical sections allow spines along the shafts of secondary dendrites to be resolved. The images shown here are projections of the stack used for reconstruction. The scale of the two images is identical. Scale bar in (H), 10 μ m.

(I) Spine densities in secondary apical dendrites of infragranular pyramidal neurons are not altered from control levels by CYC infusion.

single unit and VEP responses in CYC-infused hemispheres showed no decrement in neuronal responses, we interpret this change in the magnitude of the intrinsic imaging signal as a consequence of changes in the hemodynamic response rather than changes in neural firing rates.

Neuronal Morphology in CYC-Infused V1

Gross changes in cortical lamination were not evident in bisbenzimidazole-stained sections of CYC-infused cortex (Figure 1B), but this staining technique does not allow the morphology of individual neurons to be examined. We made use of green fluorescent protein (GFP)-

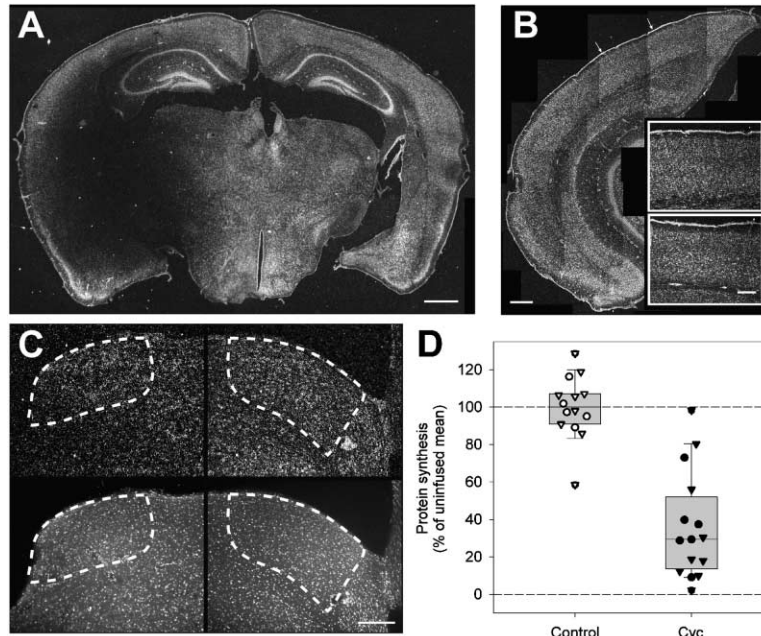


Figure 6. Thalamic Cycloheximide Infusion Inhibits LGN Protein Synthesis

(A) Cycloheximide infusion suppresses LGN protein synthesis in the infused hemisphere (left hemisphere), but not ipsilateral V1 (caudal to plane of this section, see [B] below) or contralateral LGN (right hemisphere). Scale bar, 1 mm.

(B) Thalamic CYC infusions do not reduce protein synthesis in the ipsilateral visual cortex. The section shown is from the infused hemisphere shown in (A); scale bar, 500 μ m. Insets show high-power view of a portion of the visual cortex from the same section (top inset; arrows in low-power view show the region magnified) and from the contralateral, noninfused hemisphere (bottom inset) for comparison. Inset scale bar, 200 μ m.

(C) High-magnification photographs of silver grains representing nascent protein synthesis (top) in the LGN of the cycloheximide-infused hemisphere (left) and the contralateral LGN (right; extent of each LGN is indicated with broken white line). Bisbenzimidazole staining in the same coronal sections is shown below. The section is the same as that shown in (A) above. Scale bar, 500 μ m.

(D) Quantification of protein synthesis inhibition

in the LGN (uninfused, $n = 14$ sections, two hemispheres; cycloheximide infused, $n = 15$ sections, two hemispheres). Each symbol represents a silver grain density derived from a single section; different symbols represent sections from different individual animals. Box plots represent median values, 10th, 25th, 75th, and 90th percentiles.

expressing mice to investigate potential CYC-induced morphological changes at a finer scale. These mice express GFP driven by a *thy1* promoter in a select population of cortical neurons (Feng et al., 2000); in the visual cortex of the particular strain used in this study, these are largely confined to infragranular pyramidal neurons. Comparison of individual layer V pyramidal neurons in five CYC- and five saline-infused hemispheres did not reveal any gross differences in neural morphology resulting from protein synthesis inhibition (Figures 5E and 5F). To approach this issue quantitatively, we measured dendritic spine density in these neurons by counting, in serial 0.5 μ m confocal optical sections, the number of spines per unit length along secondary dendrites that emerged from the apical dendrite (spine density along secondary, rather than primary, dendrites were measured because primary dendrites in mice possess very few spines). Spine density did not differ between CYC- and saline-infused animals (Figure 5I; mean density in CYC-infused = 0.64 ± 0.04 spines/ μ m; saline-infused = 0.61 ± 0.04 spines/ μ m; $p = 0.60$). These results provide a more complete picture of neuronal morphology following CYC infusion and together with results in shown in Figure 1B, suggest that cortical architecture and neuronal morphology are preserved intact after protein synthesis inhibition.

Intact Ocular Dominance Plasticity following Geniculate Protein Synthesis Inhibition

Visual information from the retina is communicated to the visual cortex through the LGN of the thalamus. The thalamic neurons extending afferents to the visual cortex are not, however, passive relay elements. During MD, thalamocortical afferents undergo dramatic activity-dependent rearrangements, including extensive pruning

of deprived eye arbors, and complementary expansion of nondeprived eye afferents (Antonini and Stryker, 1993). We performed a second set of experiments, then, in which we probed the thalamic contribution to rapid plasticity induced by brief MD. Selective suppression of protein synthesis within the presynaptic element of the thalamocortical circuit was attained by infusing cycloheximide into the diencephalon near the LGN, enabling us to dissect the pre- and postsynaptic contributions to the earliest expression of ocular dominance plasticity.

Cannulae-infusing cycloheximide were placed anterior to the LGN, which allowed us to selectively suppress protein synthesis in the LGN without affecting translation in V1. Peri-thalamic infusion resulted in a large sphere of protein synthesis inhibition that included much of the LGN in the infused hemisphere, but did not extend into the overlying visual cortex (Figure 6B) or the contralateral thalamus (Figure 6A). Quantification of relative levels of protein synthesis in serial sections of infused hemispheres revealed substantially reduced protein synthesis levels, which averaged $36\% \pm 7\%$ (relative to uninfused; significantly different from uninfused, $p < 0.0001$; t test) over the entire volume of the LGN (Figure 6D). Though caudal sections of the geniculate showed less suppression of protein synthesis, the central core of the LGN, which projects to the binocular region of V1 investigated in this study, showed reliable inhibition. Protein synthesis levels in V1 of infused and uninfused hemispheres were comparable (protein synthesis in V1 of infused hemisphere = $106\% \pm 3.3\%$ of uninfused hemisphere; $p = 0.14$; t test), supporting the notion that thalamic cycloheximide infusion did not block protein synthesis in postsynaptic cortical neurons.

Despite substantial inhibition of LGN protein synthesis, ocular dominance plasticity was normal in CYC-

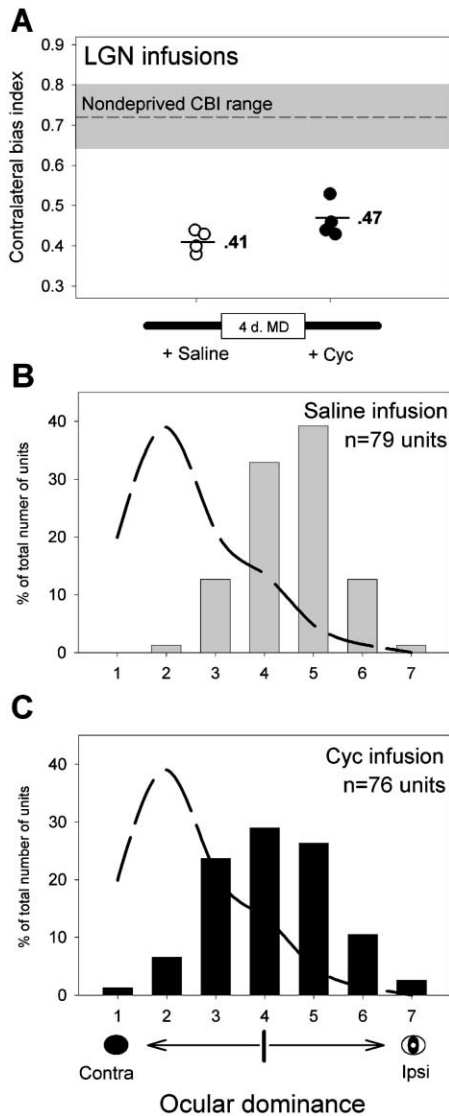


Figure 7. Ocular Dominance Plasticity Is Intact after Thalamic Infusion of Cycloheximide

(A) CBI values well outside of the normal range for nondeprived animals (gray strip) indicates saline- ($n = 4$) and cycloheximide-infused ($n = 4$) animals both show robust plasticity in response to 4 day monocular deprivation.

(B and C) Ocular dominance histograms for saline- (gray bars) and cycloheximide-infused (black bars) animals. As in Figure 3, the broken line is a best fit line for the ocular dominance distribution of units from normal, nondeprived mice; in both (B) and (C), the distribution of individual units is shifted toward the right, and toward the open ipsilateral eye.

infused animals. The mean CBI of CYC-infused animals ($CBI = 0.47 \pm 0.02$) following MD was not significantly different from that of control saline-infused mice (Figure 7A; $CBI = 0.41 \pm 0.01$, $p = 0.09$; t test), and both groups were significantly different from nondeprived mice (both $p < 0.001$; t test). Ocular dominance histograms for both groups showed a pronounced shift in the distribution of single unit responses toward the open ipsilateral eye (Figures 7B and 7C). The results suggest an asymmetry in the contribution of pre- and postsynaptic elements

to the expression of rapid plasticity; translation of novel proteins within cell bodies of the LGN is not needed for initial changes following brief MD.

Discussion

We have demonstrated that intact cortical protein synthesis is required for ocular dominance plasticity. Moreover, the blockade of plasticity by cycloheximide is not the trivial consequence of suppressing neuronal responses, as single units and VEPs recorded in CYC-infused animals demonstrate normal neuronal responsiveness and resting activity. Two aspects of the requirement for protein synthesis—its timing and locus—have interesting implications for the molecular mechanisms that mediate ocular dominance plasticity.

Rapid Structural Change in Ocular Dominance Plasticity

The timing of the requirement for protein synthesis following monocular occlusion is rapid, as suppression of cortical translation blocks the earliest plasticity apparent following monocular occlusion. While anatomical changes induced in thalamocortical arbors might well be expected to require protein synthesis for their expression, the finding that cortical protein synthesis blocks even the most rapidly expressed effects of MD is surprising. Characterizations of both the electrophysiological and anatomical dimensions of activity-dependent plasticity in a single system are rare, but evidence from studies of gill withdrawal sensitization in *Aplysia* (Bailey et al., 1992), hippocampal LTP (Engert and Bonhoeffer, 1999), and memory formation in chicks (Rose and Stewart, 1999) converge in suggesting that protein synthesis is required for structural changes that underlie “late” stages of plasticity, but *not* for the quick electrophysiological changes that precede them. Our finding of a requirement for protein synthesis in rapid ocular dominance plasticity suggests this electrophysiological plasticity may also have a structural substrate, and in this regard, may be akin to the “late” stages of other forms of plasticity.

While we have interpreted the effect of protein synthesis inhibition in ocular dominance plasticity as blocking the structural rearrangement of anatomical connections, it is possible that the effect of protein synthesis inhibition operates at a much finer scale, for example at that of the synapse or even at that of individual molecules. While this may be true, it seems very likely that large structural rearrangements of axonal/dendritic arbors would require protein synthesis, and accumulating evidence suggest that such large-scale structural changes can occur with the speed necessary to account for the effects of brief MD (Trachtenberg and Stryker, 2001).

If anatomical changes indeed contribute to the rapid changes induced by MD, this must be reconciled with much evidence documenting the relatively slow emergence of anatomical changes that substantially lag electrophysiological plasticity. In the cat, electrophysiological plasticity is apparent after hours of MD (as few as 4–6 hours) (Movshon and Dursteler, 1977; Freeman and Olson, 1982; Frank et al., 2001), while a full week of MD is required for consistent expression of changes in thalamocortical arbors (Antonini and Stryker, 1993). Nor

are more rapid changes evident in the fine structure of thalamocortical terminals: the density of thalamocortical terminals is not changed by MD (Silver and Stryker, 1999). In the mouse, the disparity in the timing of electrophysiological and anatomical change is even greater. Four days of MD drive electrophysiological plasticity to near saturating levels, but weeks of MD (between 20 and 40 days) are necessary for the emergence of significant changes in geniculocortical afferents of deprived mice (Antonini et al., 1999). Slow anatomical plasticity that greatly lags electrophysiological change is not necessarily an intrinsic property of anatomical plasticity, however. Recent experiments in the cat suggest that a rapid time course for structural change is plausible—dramatic anatomical changes in corticocortical connections are apparent with only 2 days of strabismus (Trachtenberg and Stryker, 2001). Thus, it seems likely that anatomical change can arise shortly after MD begins and may contribute to rapid plasticity, as our data suggest. The notion of generally slow, lagging anatomical plasticity likely has much to do with assumptions about the locus of initial plasticity, which is discussed further below.

A Cortical Locus for Rapid Ocular Dominance Plasticity

Suppression of cortical protein synthesis blocks the effects of MD, while substantial reduction of protein synthesis in the LGN leaves ocular dominance plasticity intact. While cortical cycloheximide infusion would likely disrupt translation in thalamocortical axon terminals, there is, to our knowledge, little evidence of protein synthesis machinery in the axon terminals of mammalian CNS neurons. Thus, the requirement for protein synthesis is likely to be confined to the postsynaptic, cortical element of the thalamocortical circuit. These findings suggest that the most rapid effects of MD are subserved by structural changes in cortical neurons, which shape subsequent plasticity in thalamocortical afferents.

Two caveats to this interpretation bear consideration. First, we cannot rule out the possibility that transient, translation-independent changes in thalamocortical axon terminals contribute to the most rapid effects of MD. Second, it is possible that protein synthesis in the LGN is required for rapid ocular dominance plasticity, but the low levels of translation that persist following cycloheximide infusion into the LGN are sufficient to mediate plasticity. This appears unlikely, as geniculate cycloheximide infusions more fully blocked protein synthesis than did cortical infusions, which prevented ocular dominance plasticity. A more parsimonious explanation of our data suggests a cortical locus for the most rapid plasticity following MD.

Ocular Dominance Plasticity: Balancing Mechanisms for Stability and Speed

If cortical changes are indeed primary in mediating ocular dominance plasticity, then lagging changes in thalamocortical arbors are expected and do not reflect any intrinsically slow mechanisms subserving anatomical change. One possibility is that thalamocortical changes are instructed by cortical plasticity and therefore necessarily lag cortical remodeling, which may itself be subserved by structural changes. In this model, thalamocor-

tical arbors may be viewed as an enduring and stable base upon which rapid changes in cortical connections can be implemented. Ocular dominance plasticity would then be subserved by a two-tiered system of synaptic change in which dynamic cortical networks promote rapid plasticity, while thalamocortical networks provide both stability and the means to amplify initial cortical changes. Data from a recent study of rapid physiological plasticity following MD in the cat provide strong evidence for this model by showing that the earliest shifts in ocular dominance are confined to cortical layers outside thalamorecipient layer IV (Trachtenberg et al., 2000).

Which Proteins Are Translated?

Our results point to a central remaining question: namely, which proteins must be translated for structural rearrangements to occur in ocular dominance plasticity? Numerous transcription factors show activity-dependent regulation, and presumably some of their target molecules participate in altering synaptic architecture. A number of promising candidates in this group have been identified and include the adhesion protein N-cadherin, which is upregulated by activity and necessary for late, but not early, phases of *in vitro* plasticity (Bozdagi et al., 2000) and the protease tissue plasminogen activator, which exhibits activity-dependent translation (Qian et al., 1993) and is required for ocular dominance plasticity in mice (N. Mataga and T. Hensch, personal communication) and cats (Muller and Griesinger, 1998).

Experimental Procedures

Monocular Deprivation

MD was performed according to published protocols (Gordon and Stryker, 1996), except 3% isofluorane (Abbott, North Chicago, IL) in oxygen was used for anesthesia. In every case, MD was initiated within the critical period for mouse ocular dominance (p26–p30) and lasted for 4 days.

Surgical Implantation of Minipumps

Mice were anesthetized with 3% isofluorane in oxygen and mounted in a stereotaxic holder. Ophthalmic lubricant was applied to protect the eyes, and body heat maintained at 37°C with a heating pad. For infusion experiments, Alzet osmotic minipumps (Alza 1002, 0.25 μ l/hr) were filled either with cycloheximide (10 mg/ml; Sigma, St. Louis, MO) or with physiological saline for control experiments and attached to 30G stainless steel cannulae. Under aseptic conditions, a longitudinal incision was made in the scalp over the mid-sagittal sinus, and the skin retracted. The portions of the skull overlying occipital and frontal portions of the brain were cleaned and dried. To aid in securing the cannula, a single skull screw was implanted approximately 2 mm lateral of the midline and 2 mm caudal of bregma in the skull overlying the noninfused hemisphere. Cannulae were implanted using stereotaxic coordinates (V1 infusion coordinates: 1 mm lateral (midline), 1 mm rostral (λ), 1 mm deep; LGN infusion coordinates: 1.3 mm lateral, 0.7 mm caudal, 2.5 mm deep) and were secured to the skull and skull screw with dental cement. The attached minipump was placed in a subcutaneous pocket at the nape of the neck. The scalp was closed over the implant, and the animal returned to its home cage when sternal. For plasticity experiments, minipump implantation was performed on the day prior to MD, and infusion continued for the duration of the MD, for a total of 5 days of infusion. For autoradiography experiments and quantitative measurements of receptive field properties, implantation was performed in p25–p30 mice, and infusion lasted 5 days.

Single Unit Recording

All monocularly deprived mice were prepared for electrophysiology after 4 days of MD during the peak of the critical period for ocular dominance plasticity (p26–p30); thus, single unit recording took place in these mice at 30–34 days of age. Data shown in the “No MD” column of Figure 3A was derived from two critical period age mice (ages in days = 30 and 31) as well as four older mice (ages = 43, 45, 50, and 77), as there is no developmental change in CBI values of nondeprived mice (Antonini et al., 1999). Mice were anesthetized for electrophysiological recording with a combination of Nembutal (Abbott; 50 mg/kg) and chlorprothixene (Sigma; 0.2 mg) using standard protocols (Gordon and Stryker, 1996). In each mouse, single units were isolated at intervals of 60 μ m or more, using lacquer coated tungsten electrodes in the binocular region of V1 (in mice receiving infusions, 2.1–2.6 mm from the cannula site) contralateral to the deprived eye. A handlamp was used to project moving bars or squares onto a tangent screen to drive neuronal responses. The balance of the two eyes’ input to each unit was scored on the 1 to 7 scale of Hubel and Wiesel (Hubel and Wiesel, 1962), where a value of 1 indicates complete domination by the contralateral eye, and 7 indicates input arises from the ipsilateral eye only. For each mouse, these ocular dominance scores were used to compute a single contralateral bias index (CBI) according to the formula

$$\text{CBI} = [(n_1 - n_7) + (2/3)(n_2 - n_6) + (1/3)(n_3 - n_5) + N]/2N,$$

where N = total number of cells, and n_x = number of cells with ocular dominance scores equal to x. Each unit was also scored for habituation on a 0 (no habituation) to 3 (prolonged and rapid habituation) scale and for the presence of orientation bias, assessed as “present” when the response to a light bar swept at the preferred orientation exceeded that of a light bar swept at the orthogonal orientation.

Quantitative Measurement of Single Unit Responses

A total of six critical period age mice (three CYC-infused and three saline-infused) were used in quantitative measures of spike rates. Single unit responsiveness was assessed using computer-driven stimulus presentation and spike collection. Stimulus-driven neuronal responses were elicited by a high-contrast (90%), low-spatial frequency (0.04 cyc/deg) square wave grating flashed at 1 Hz at the optimal orientation. Responses to this stimulus were integrated over 100 ms bins to determine the maximum firing frequency. Spontaneous rates of activity were calculated as the mean spike rates averaged over two trials in which no stimulus was presented. The histograms of response latency (Figure 4B) were generated by integrating responses over 25 ms bins, normalizing response amplitude to the maximal spike rate, and plotting responses as a function of time from stimulus onset.

VEP Recording

A total of six mice were used in VEP recordings; three of these were p30–p34 wild-type mice, and three were adult GFP mice (used for studies of single neuron morphology, as described below). Data from these two groups were pooled, as there was no difference in their mean VEP amplitude ($p = 0.29$; t test). Each mouse received bilateral cortical infusions, with CYC delivered to one hemisphere and saline to the other. After 5 days of bilateral infusion, mice were anesthetized for VEP recordings as outlined above for single unit recordings. VEP signals were recorded using tungsten microelectrodes and amplified with bandpass (0.1–500 Hz) filtering. Full field flashes delivered to the eye contralateral to the hemisphere studied were used to elicit VEP responses. 60–80 stimulus presentations were averaged to generate each VEP, and these traces were smoothed with boxcar binning. Responses were quantified by measuring the peak to trough amplitude of the responses recorded at 400 μ m below the cortical surface, the depth at which responses are usually maximal (Porciatti et al., 1999).

Optical Imaging

A total of six mice were used for optical imaging of intrinsic signals; four of these were p30–p34 wild-type mice, and two were adult GFP

mice (see below). Data from these animals was pooled, as there was no difference in the peak intrinsic signal response ($p >> 0.05$ for responses in both CYC- and saline-infused hemispheres). Mice received 5 day bilateral infusions (CYC into one hemisphere and saline into the other) as described for VEP measurements above. Mice were anesthetized with a combination of urethane (Sigma; 1.5 g/kg) and chlorprothixene (Sigma; 0.2 mg). Reflectance of visual cortex (illuminated with 610 nm light) following binocular presentation of drifting, high-contrast square wave gratings (0.0125 cyc/deg, 0.14 cyc/s, 50% contrast) was captured with a cooled, slow scan CCD camera (Princeton Instruments) continuously over the period of visual stimulation (~12 min epochs) and analyzed by extracting the Fourier component of the intrinsic signal matched to the stimulus presentation rate (V. Kalatsky, personal communication). The magnitude and specificity of cortical responses are jointly represented using color (indicating retinotopic elevation) and lightness (indicating response strength), as seen in Figure 5D.

³H-Leucine Injection and Slice Preparation

Mice were anesthetized with 3% isoflurane in oxygen, and body heat maintained at 37°C with a heating pad. 100 μ Ci of tritiated leucine (1 mCi/ml, NEN Life Sciences, Boston, MA) were injected into the tail vein. Anesthesia was discontinued, and mice were allowed to survive for 30 min after righting themselves. They were then deeply anesthetized with Nembutal and perfused with cold 0.1 M phosphate buffer followed by 4% paraformaldehyde. The brain was removed and cryoprotected overnight in 4% paraformaldehyde/30% sucrose. 40 μ m coronal slices were cut on a freezing microtome, mounted from 1% gelatin onto slides, dehydrated and defatted, and allowed to dry overnight.

Autoradiography

In the darkroom, sections were coated with a thin layer of emulsion (Kodak NTB-2, Kodak Scientific Imaging Systems, New Haven, CT) by dipping. They were allowed to dry for 4 hours in a humidified chamber, then transferred to dry, light-tight boxes to be stored at 4°C for exposure. Sections were developed by serial exposure to developer, water rinse, and fixative, and bisbenzimidazole-stained before dehydrating and cover slipping.

Quantification of Protein Synthesis Inhibition and Cell Density

Silver grain puncta representing incorporation of tritium-labeled leucine into nascent proteins were counted to quantify the effects of cycloheximide infusion. All quantification of protein synthesis inhibition was carried out by comparing hemispheres (infused versus uninfused) in a single section and were therefore perfused identically and on slides exposed for the same length of time. Typically, sections were developed after 10 days, though exposures ranged in length from 6 to 21 days. To measure protein synthesis in the cortex, measurements were made in coronal sections containing portions of V1 corresponding to central areas of the visual field (~1 mm from the caudal pole of the brain). Digital photographs of fields ~350 \times 450 μ m in size were taken at ~1 mm intervals across the medial-lateral extent of the cortex. Silver grain puncta were counted using an automated particle counting function developed on the public domain NIH Image program (developed at the U.S. National Institutes of Health and available on the Internet at <http://rsb.info.nih.gov/nih-image/>) with the threshold set at an arbitrary level, which was identical for infused and uninfused hemispheres in each section. Cortical cell density was quantified using similar counting procedures in bisbenzimidazole-stained sections identical to those used for measuring protein synthesis inhibition. Measurements of protein synthesis inhibition in the LGN were made in a similar fashion, with two changes. Protein synthesis was quantified in serial sections of the LGN and therefore included the entire volume of the LGN. Also, the area encompassed by the LGN in each section was identified using cytoarchitectonic cues and the silver grain count restricted to that area.

Analysis of Neuronal Morphology Using GFP Mice

GFP mice were generously provided by Joshua Sanes (Washington University, St. Louis, MO). Images of GFP-expressing neurons were

obtained using fluorescent confocal imaging of 150 μm coronal slices of primary visual cortex. Quantitative analysis of dendritic spine density in infragranular pyramidal neurons was performed using high-power confocal images of serial optical sections (0.5 μm steps) of secondary dendrites of the apical dendrite; 15 dendrites in five CYC-infused animals and 13 dendrites in five saline-infused animals were analyzed. The trajectory of the secondary dendrite was traced using NeuroLucida software (Microbrightfield, Inc; Colchester, VT), and attached dendritic spines were identified by examining images in serial optical sections of the stack. Spine density was analyzed using NeuroExplorer (Microbrightfield, Inc.). Photographs shown in Figures 5G and 5H were generated by projecting Z-series stacks using a brightest-point algorithm in NIH Image software. Out-of-plane fluorescence was minimized in these projections by limiting the area of analysis in each section to the region containing the dendritic shaft and spines of interest.

Acknowledgments

The authors thank Jessica Hanover for participating in the data collection for Figure 3, Josh Sanes for providing GFP-expressing mice, Joshua Trachtenberg, Valery Kalatsky, Antonella Antonini, and Patrick McQuillen for their assistance with experiments and for thoughtful discussions. S.T. is an Achievement Rewards for College Scientists Foundation Scholar. This research was supported by NIH Grant NS16033 to M.P.S.

Received: September 4, 2001

Revised: March 6, 2002

References

- Androutsellis-Theotokis, A., McCormack, W.J., Bradford, H.F., Stern, G.M., and Pliego-River, F.B. (1996). The depolarization-induced release of [125I]BDNF from brain tissue. *Brain Res.* **743**, 40–48.
- Antonini, A., and Stryker, M.P. (1993). Rapid remodeling of axonal arbors in the visual cortex. *Science* **260**, 1819–1821.
- Antonini, A., Fagiolini, M., and Stryker, M.P. (1999). Anatomical correlates of functional plasticity in mouse visual cortex. *J. Neurosci.* **19**, 4388–4406.
- Bailey, C.H., and Chen, M. (1989). Time course of structural changes at identified sensory neuron synapses during long-term sensitization in *Aplysia*. *J. Neurosci.* **9**, 1774–1780.
- Bailey, C.H., Montarolo, P., Chen, M., Kandel, E.R., and Schacher, S. (1992). Inhibitors of protein and RNA synthesis block structural changes that accompany long-term heterosynaptic plasticity in *Aplysia*. *Neuron* **9**, 749–758.
- Bailey, C.H., Bartsch, D., and Kandel, E.R. (1996). Toward a molecular definition of long-term memory storage. *Proc. Natl. Acad. Sci. USA* **93**, 13445–13452.
- Barea-Rodríguez, E.J., Rivera, D.T., Jaffe, D., and Martínez, J.J. (2000). Protein synthesis inhibition blocks the induction of mossy fiber long-term potentiation in vivo. *J. Neurosci.* **20**, 8528–8532.
- Bear, M.F., Kleinschmidt, A., Gu, Q., and Singer, W. (1990). Disruption of experience-dependent synaptic modifications in striate cortex by infusion of an NMDA receptor antagonist. *J. Neurosci.* **10**, 909–925.
- Bozdagi, O., Shan, W., Tanaka, H., Benson, D.L., and Huntley, G.W. (2000). Increasing numbers of synaptic puncta during late-phase LTP: N-cadherin is synthesized, recruited to synaptic sites, and required for potentiation. *Neuron* **28**, 245–259.
- Cabelli, R.J., Hohn, A., and Shatz, C.J. (1995). Inhibition of ocular dominance column formation by infusion of NT-4/5 or BDNF. *Science* **267**, 1662–1666.
- Daw, N.W., Stein, P.S., and Fox, K. (1993). The role of NMDA receptors in information processing. *Annu. Rev. Neurosci.* **16**, 207–222.
- Dubnau, J., and Tully, T. (1998). Gene discovery in *Drosophila*: new insights for learning and memory. *Annu. Rev. Neurosci.* **21**, 407–444.
- Engert, F., and Bonhoeffer, T. (1999). Dendritic spine changes associated with hippocampal long-term plasticity. *Nature* **399**, 66–70.

- Feng, G., Mellor, R.H., Bernstein, M., Keller-Peck, C., Nguyen, Q.T., Wallace, M., Nerbonne, J.M., Lichtman, J.L., and Sanes, J.R. (2000). Imaging neuronal subsets in transgenic mice expressing multiple spectral variants of GFP. *Neuron* **28**, 41–51.
- Flexner, J.B., Flexner, L.B., and Stellar, E. (1963). Memory in mice as affected by intracerebral puromycin. *Science* **141**, 57–59.
- Frank, M.G., Issa, N.P., and Stryker, M.P. (2001). Sleep enhances plasticity in the developing visual cortex. *Neuron* **30**, 275–287.
- Freeman, R.D., and Olson, C. (1982). Brief periods of monocular deprivation in kittens: effects of delay prior to physiological study. *J. Neurophysiol.* **47**, 139–149.
- Frey, U., Krug, M., Reymann, K.G., and Matthies, H. (1988). Anisomycin, an inhibitor of protein synthesis, blocks late phases of LTP phenomena in the hippocampal CA1 region in vitro. *Brain Res.* **452**, 57–65.
- Gillespie, D.C., Crair, M.C., and Stryker, M.P. (2000). Neurotrophin-4/5 alters responses and blocks the effect of monocular deprivation in cat visual cortex during the critical period. *J. Neurosci.* **20**, 9174–9186.
- Gordon, J.A., and Stryker, M.P. (1996). Experience-dependent plasticity of binocular responses in the primary visual cortex of the mouse. *J. Neurosci.* **16**, 3274–3286.
- Gordon, J.A., Cioffi, D., Silva, A.J., and Stryker, M.P. (1996). Deficient plasticity in the primary visual cortex of α -calcium/calmodulin-dependent protein kinase II mutant mice. *Neuron* **17**, 491–499.
- Hanover, J.L., Huang, Z.J., Tonegawa, S., and Stryker, M.P. (1999). Brain-derived neurotrophic factor overexpression induces precocious critical period in mouse visual cortex. *J. Neurosci.* **19**, RC40.
- Hensch, T.K., Fagiolini, M., Mataga, N., Stryker, M.P., Baekkeskov, S., and Kash, S.F. (1998). Local GABA circuit control of experience-dependent plasticity in developing visual cortex. *Science* **282**, 1504–1508.
- Hubel, D.H., and Wiesel, T.N. (1962). Receptive fields, binocular interaction and functional architecture in the cat's visual cortex. *J. Physiol.* **160**, 106–154.
- Huber, K.M., Kayser, M.S., and Bear, M.F. (2000). Role for rapid dendritic protein synthesis in hippocampal mGluR-dependent long-term depression. *Science* **288**, 1254–1256.
- Kennedy, C., Suda, S., Smith, C.B., Miyaoka, M., Ito, M., and Sokoloff, L. (1981). Changes in protein synthesis underlying functional plasticity in immature monkey visual system. *Proc. Natl. Acad. Sci. USA* **78**, 3950–3953.
- Krug, M., Lossner, B., and Ott, T. (1984). Anisomycin blocks the late phase of long-term potentiation in the dentate gyrus of freely moving rats. *Brain Res. Bull.* **13**, 39–42.
- Kurontani, T., Higashi, S., Inokawa, H., and Toyama, K. (1996). Protein and RNA synthesis dependent and independent LTPs in developing rat visual cortex. *Neuroreport* **8**, 35–39.
- Lein, E.S., and Shatz, C.J. (2000). Rapid regulation of brain-derived neurotrophic factor mRNA within eye-specific circuits during ocular dominance column formation. *J. Neurosci.* **20**, 1470–1483.
- Levenes, C., Daniel, H., and Crépel, F. (1998). Long-term depression of synaptic transmission in the cerebellum: cellular and molecular mechanisms revisited. *Prog. Neurobiol.* **55**, 79–91.
- Linden, D.J. (1996). A protein synthesis-dependent late phase of cerebellar long-term depression. *Neuron* **17**, 483–490.
- Mayford, M., and Kandel, E.R. (1999). Genetic approaches to memory storage. *Trends Genet.* **15**, 463–470.
- McAllister, A.K., Lo, D.C., and Katz, L.C. (1995). Neurotrophins regulate dendritic growth in developing visual cortex. *Neuron* **15**, 791–803.
- Movshon, J.A., and Dursteler, M.R. (1977). Effects of brief periods of unilateral eye closure upon the kitten's visual system. *J. Neurophysiol.* **40**, 1255–1265.
- Muller, C.M., and Griesinger, C.B. (1998). Tissue plasminogen activator mediates reverse occlusion plasticity in visual cortex. *Nat. Neurosci.* **1**, 47–53.
- Olson, C.R., and Freeman, R.D. (1980). Cumulative effect of brief

- daily periods of monocular vision on kitten striate cortex. *Exp. Brain Res.* **38**, 53–56.
- Pham, T.A., Impey, S., Storm, D.R., and Stryker, M.P. (1999). CRE-mediated gene transcription in neocortical neuronal plasticity during the developmental critical period. *Neuron* **22**, 63–72.
- Porciatti, V., Pizzorusso, T., and Maffei, L. (1999). The visual physiology of the wild-type mouse determined with pattern VEPs. *Vision Res.* **39**, 3071–3081.
- Qian, Z., Gilbert, M.E., Colicos, M.A., Kandel, E.R., and Kuhl, D. (1993). Tissue-plasminogen activator is induced as an immediate-early gene during seizure, kindling and long-term potentiation. *Nature* **361**, 453–457.
- Reiter, H.O., and Stryker, M.P. (1988). Neural plasticity without post-synaptic action potentials: less-active inputs become dominant when kitten visual cortical cells are pharmacologically inhibited. *Proc. Natl. Acad. Sci. USA* **85**, 3623–3627.
- Reiter, H.O., Waitzman, D.M., and Stryker, M.P. (1986). Cortical activity blockade prevents ocular dominance plasticity in the kitten visual cortex. *Exp. Brain Res.* **65**, 182–188.
- Roberts, E.B., Meredith, M.A., and Ramoa, A.S. (1998). Suppression of NMDA receptor function using antisense DNA blocks ocular dominance plasticity while preserving visual responses. *J. Neurophysiol.* **80**, 1021–1032.
- Rose, S.P.R., and Stewart, M.G. (1999). Cellular correlates of stages of memory formation in the chick following passive avoidance training. *Behav. Brain Res.* **98**, 237–243.
- Schoups, A.A., Elliott, R.C., Friedman, W.J., and Black, I.B. (1995). NGF and BDNF are differentially modulated by visual experience in the developing geniculocortical pathway. *Brain Res.* **86**, 326–334.
- Shaw, C., and Cynader, M. (1984). Disruption of cortical activity prevents ocular dominance changes in monocularly deprived kittens. *Nature* **308**, 731–734.
- Silver, M.A., and Stryker, M.P. (1999). Synaptic density in geniculocortical afferents remains constant after monocular deprivation in the cat. *J. Neurosci.* **19**, 10829–10842.
- Soderling, T.R. (2000). CaM-kinases: modulators of synaptic plasticity. *Curr. Opin. Neurobiol.* **10**, 375–380.
- Trachtenberg, J.T., and Stryker, M.P. (2001). Rapid anatomical plasticity of horizontal connections in the developing visual cortex. *J. Neurosci.* **21**, 3476–3482.
- Trachtenberg, J.T., Trepel, C., and Stryker, M.P. (2000). Rapid extragranular plasticity in the absence of thalamocortical plasticity in the developing primary visual cortex. *Science* **287**, 2029–2032.
- Wiesel, T.N., and Hubel, D.H. (1963). Single cell responses in striate cortex of kittens deprived of vision in one eye. *J. Neurophysiol.* **26**, 1003–1017.
- Wu, L., Wells, D., Tay, J., Mendis, D., Abbott, M., Barnitt, A., Quinlan, E., Heynen, A., Fallon, J.R., and Richter, J.D. (1998). CPEB-mediated cytoplasmic polyadenylation and the regulation of experience-dependent translation of α -CaMKII mRNA at synapses. *Neuron* **21**, 1129–1139.
- Zafra, F., Lindholm, D., Castrén, E., Hartikka, J., and Thoenen, H. (1992). Regulation of brain-derived neurotrophic factor and nerve growth factor mRNA in primary cultures of hippocampal neurons and astrocytes. *J. Neurosci.* **12**, 4793–4799.